JCTC Journal of Chemical Theory and Computation

Article

pubs.acs.org/JCTC

A Polarizable and Transferable PHAST N_2 Potential for Use in Materials Simulation

Christian R. Cioce,*[,†] Keith McLaughlin,[†] Jonathan L. Belof,[‡] and Brian Space[†]

[†]Department of Chemistry, University of South Florida, 4202 E. Fowler Ave., CHE205, Tampa, Florida 33620-5250, United States

[‡]Lawrence Livermore National Laboratory, 7000 East Ave., Livermore, California 94550, United States

ABSTRACT: A polarizable and transferable intermolecular potential energy function, potentials with high accuracy, speed, and transferability (PHAST), has been developed from first principles for molecular nitrogen to be used in the modeling of heterogeneous processes such as materials sorption and separations. A five-site (van der Waals and point charge) anisotropic model, that includes many-body polarization, is proposed. It is parametrized to reproduce high-level electronic structure calculations (CCSD(T) using Dunning-type basis sets extrapolated to the CBS limit) for a representative set of dimer potential energy curves. Thus it provides a relatively simple yet robust and broadly applicable representation of nitrogen. Two versions are developed, differing by the type of mixing rules applied to unlike Lennard-Jones potential sites. It is shown that the Waldman–Hagler mixing rules are more accurate than Lorentz–Berthelot. The resulting potentials are demonstrated to be effective in modeling neat nitrogen but are designed to also be useful in modeling N_2 interactions in a large array of environments such as metal–organic frameworks and zeolites and at interfaces. In such settings, capturing anisotropic forces and interactions with (open and coordinated) metals and charged/polar environments is essential. In developing the potential, it was found that adding a seemingly redundant dimer orientation, slip-parallel (**S**), improved the transferability of the potential energy surface (PES). Notably, one of the solid phases of nitrogen was not as accurately represented energetically without including S in the representative set. Liquid simulations, however, were unaffected and worked equally well for both potentials. This suggests that accounting for a wide variety of configurations is critical in designing a potential that is intended for use in heterogeneous environments where many orientations, including those not commonly explored in the bulk, are possible. Testing and validation of the potential are achieved via simulations of a thermal distribution of trimer geometries compared to analogous high level electronic structure calculations and molecular simulations of bulk pressure–density isotherms across the vapor, supercritical, and liquid phases. Crystal lattice parameters and energetics of the α-N_2 and γ-N_2 solid phases are also evaluated and determined to be in good agreement with experiment. Thus the proposed potential is shown to be efficacious for gas, liquid, and solid use, representing both disordered and ordered configurations.

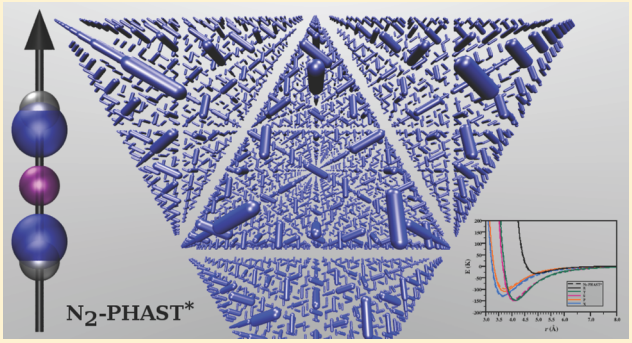

INTRODUCTION

Dinitrogen, N_2, is a major component of the Jovian planets and their moons, such as Saturn and Titan as well as Neptune and Triton. Here on Earth, N_2 is the most abundant constituent of air, comprising roughly 78% of it along with oxygen, water vapor, and other trace gases. Thus, nitrogen plays a critical role in many energy, environmental, and life processes. Given its ubiquity and relative inertness, separating it efficiently and completely from other molecular species, such as methane and CO_2, is a useful goal.[1,2]

Metal–organic frameworks (MOFs) are promising platforms to achieve efficient and cost-effective separations of a variety of gases. There is particular urgency in applying MOFs to energy-related processes, including associated separations, given the need for increased energy production in an environmentally sustainable fashion. MOFs consist of metal ions coordinated to organic linkers;[3] these materials can present large (chemically and physically) tunable surface areas and topologies that result in specific and selective molecular interactions.[4−7] As a result, MOFs have shown utility for a multitude of purposes, including molecular capture, storage, catalysis, and separation.[1,2,7,8]

Given their ability to preferentially sorb CO_2 over N_2[7,9−11] or CH_4 over N_2, for example, even in humid environments, MOFs are realistic solutions to many of the green challenges faced today. Molecular simulations now play an essential role in helping to both predict and retrodict material properties and processes that are determined empirically.[7] Simulation is capable of both designing and improving material/MOF functionality by elucidating essential sorbent–sorbate interactions.[12] In order for simulation to play a central role, accurate and transferable potential energy functions must be available; high fidelity descriptions of small molecule potential energy surfaces (PESs), when available, are usually expressed in

Received: June 20, 2013
Published: November 15, 2013

   dx.doi.org/10.1021/ct400526a | *J. Chem. Theory Comput.* 2013, 9, 5550−5557

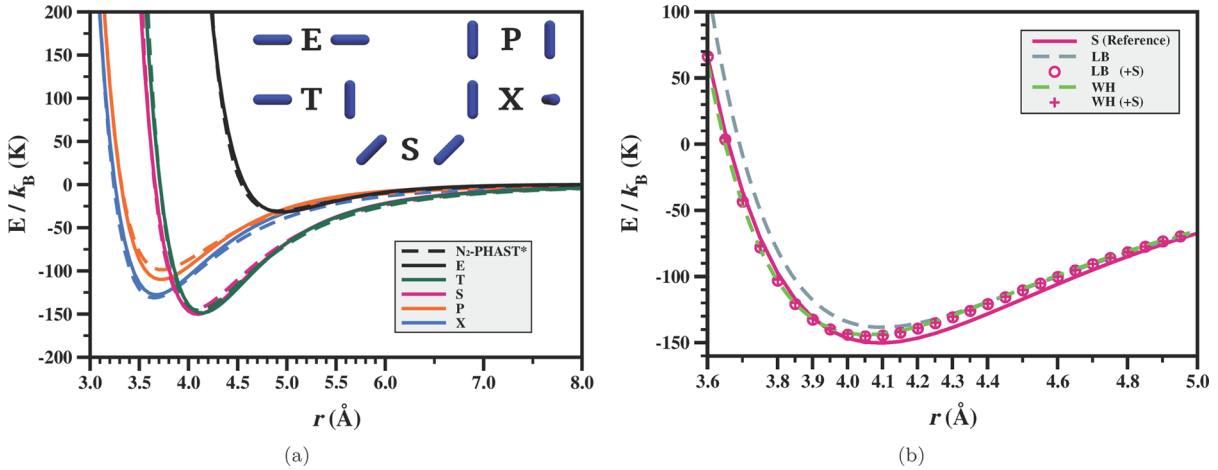

Figure 1. (a) The reference Born−Oppenheimer potential surface of the N_2 dimer (solid lines), calculated at the CCSD(T) level of theory, along with the N_2-PHAST* potential (dashed lines). The illustrated polar potential makes use of the WH mixing rules, however the LB results are visually indistinguishable. Additionally, the five corresponding representative dimer orientations, labeled **E** (end-to-end), **T** (T-configuration), **S** (slip-parallel), **P** (parallel), and **X** (X-configuration), are shown. (b) The ab initio reference S potential curve from (a) (solid pink line) along with the calculated curves via the N_2-PHAST* model, both before (dashed lines) and after (pink symbols) the inclusion of this orientation in the dimer set. It can be seen that including this configuration results in a closer mapping to the reference, an effect independent of the mixing rule applied. It will be shown below that only the potentials that included the S configuration in their construction are highly transferable.

complex forms unsuitable for simulations where unlike species interact.[13,14] Building on our previous work describing MOF and sorbate (e.g., H_2, CO_2, and CH_4) force fields,[7,15−21] a transferable and polarizable potential energy function for dinitrogen, N_2-PHAST* (potentials with high accuracy, speed, and transferability), has been developed. It is parametrized to high level ab initio data (CCSD(T) using Dunning-type basis sets extrapolated to the CBS limit) and constructed for use in heterogeneous environments, such as MOFs and planar interfaces, or more generally where polarization and specific anisotropic interactions cannot be ignored. Typical liquid-state potential surfaces are fit to bulk properties and can be highly effective in like environments or mixtures where the neat bulk-like orientations are still prevalent.[22−24] As a result, the region of applicability of such force fields reflects the typical orientations dominant in that phase. In contrast, molecular sorption at interfaces, both planar and sorbate/solid, tends to explore a wider range of configuration space and thus requires a potential that is effective for the entire range of molecular orientations and interactions associated with highly heterogeneous environments. Thus, the form of our potential is chosen to be compact and reasonably simple to implement yet sufficiently accurate, containing electrostatic, repulsion/dispersion, and explicit induction contributions to the total energy. Note, constructing transferable potentials for such applications is an active area of investigation.[25] Murthy et al. developed a five charge site model for solid-state simulation in 1983, namely 5*q*, which contains electrostatic and repulsion/dispersion contributions to the total energy.[26] This potential is similar to the nonpolar variant of our model, N_2-PHAST, though it will be shown that our models outperform it.

The remainder of this article is outlined as follows: we next present the form of our potential in greater detail, offering a short review of the Thole−Applequist-type polarization models, then discuss the parametrization process, and last transition to the validation of the potential.

METHODS

Born−Oppenheimer Potential Surface. The nitrogen molecule was approximated as rigid with a bond length of 1.098 Å, as determined by experiment.[27,28] Note, it is simple to relax this constraint and include full flexibility,[29,30] but this was not done here. To construct the Born−Oppenheimer potential surface for N_2−N_2, five dimer orientations were selected as representative of the geometries and energetics explored by nitrogen in the condensed phase, namely, **E** (end-to-end), **T** (T-configuration), **S** (slip-parallel), **P** (parallel), and **X** (X-configuration) (see Figure 1a).[18,31,32] For each orientation, the pair energies were calculated for center-of-mass distances *r* apart along the *z*-axis. In the domain spanning *r* = 3.00−8.00 Å, energies were calculated every Δ0.05 Å. All ab initio calculations were performed using Molpro[33] at the CCSD(T)[34] level of theory, unless otherwise stated. The employed basis functions were the augmented correlation-consistent sets of Dunning et al. (aug-cc-pVTZ/QZ).[35,36] Basis set superposition errors were counterpoise-corrected via the method of Boys and Bernardi,[37] and the energy eigenvalues extrapolated to the complete basis set (CBS) limit in a standard fashion.[38] The PESs including (Figure 1a) and neglecting (not shown) the slip-parallel (**S**) orientation both nearly exactly reproduce the high-accuracy CCSD(T) reference calculation. However, even though **S** is only a seemingly small orientational change from the already-included dimer configurations, it is not predicted as accurately unless explicitly included in the reference set; Figure 1b demonstrates this effect. It will be shown below that this does not change simulated liquid-state data but has a large effect on the solid-state energetics where the **S** configuration is relevant. Thus including the **S** configuration appears to be essential in constructing a highly transferable potential. This suggests that it is critical for the representative set of orientations to be comprehensive in order to develop potentials for use in heterogeneous media, where parts of configuration space that are not important for neat liquid simulations may be explored, such as simulating sorption in porous media. Note, it is also possible to include a large set of random dimers in a representative PES set.[39]

Many-Body Polarization. A highly transferable potential energy function for use in charged/polar heterogeneous environments requires inclusion of induction effects which typically demand a many-body treatment. Thus a point atomic polarizability model of the Thole−Applequist-type was adopted. A brief description of such polarization models, as applied here, is presented first. A more thorough description can be found elsewhere.[17,40−43] In such models, subjecting a collection of bodies with nonzero static point polarizabilities α (that after interaction become polarizability tensors on each site) to a static electric field E induces a dipole moment:

$$u_i^m = \alpha_i(E_i^m + E'^m_i) \tag{1}$$

$$u_i^m = \alpha_i\left(E_i^m - \sum_{j,n} T_{ij}^{mn} u_j^n\right) \tag{2}$$

where lower indices label the sites, upper indices label the vector/tensor components, T is the exponentially damped dipole field tensor, and E' is the induced electric field. With some manipulation, one finds the $3N \times 3N$ matrix equation:

$$\sum_{j,n}\left(\frac{1}{\alpha_i}\delta_{ij}\delta^{mn} + T_{ij}^{mn}\right)u_j^n = E_i^m \tag{3}$$

from which one may construct block matrices:

$$\hat{\mathbf{A}} \equiv \begin{pmatrix} \left[\frac{I}{\alpha_0}\right] & [T_{0,1}] & \cdots & [T_{0,N-1}] \\ [T_{1,0}] & \left[\frac{I}{\alpha_1}\right] & \cdots & [T_{1,N-1}] \\ \cdots & \cdots & \cdots & \cdots \\ [T_{N-1,0}] & [T_{N-1,1}] & \cdots & \left[\frac{I}{\alpha_{N-1}}\right] \end{pmatrix} \tag{4}$$

$$\mathbf{u} = \begin{pmatrix} [u_0] \\ [u_1] \\ \cdots \\ [u_{N-1}] \end{pmatrix} \quad \mathbf{E} = \begin{pmatrix} [E_0] \\ [E_1] \\ \cdots \\ [E_{N-1}] \end{pmatrix} \tag{5}$$

leading to

$$\hat{\mathbf{A}}\mathbf{u} = \mathbf{E} \tag{6}$$

which has solutions by either matrix inversion or iterative methods; the latter being used herein.

Finally, the polarization energy is given by

$$U_{\text{pol}} = -\frac{1}{2}\sum_{i,m} u_i^m E_i^m \tag{7}$$

Long-range corrections are handled using an implementation of the Wolf field method, which we have recently shown to be efficient and effective.[17,44] The polarizability model has the advantage that it can incorporate polarizable sites from any other species (e.g., material or other sorbent) that is similarly parametrized to gas-phase data, without further assumptions. The ostensible disadvantage is the cost of evaluating the many-body function. However, this can be largely offset by iterating efficiently and porting these operations to graphics processing units or GPUs.[15,45]

Potential Energy Function. The nitrogen potential model is referred to as N_2-PHAST*, where N_2 signifies nitrogen, * denotes the inclusion of explicit polarization, and PHAST is a newly defined acronym which refers to the form of our growing group of broadly applicable potential energy functions.[17,18,20,21] We additionally define a distinguishable model which neglects polarization effects, N_2-PHAST, for comparative purposes. Suitable for both molecular dynamics and Monte Carlo simulations, the PHAST potential has been designed with transferability in mind by explicitly including all essential potential energy interactions encountered in describing complex systems from the gas to solid phases. The form of our potential includes contributions to the many-body polarization, electrostatic, and the electronic repulsion/dispersion energy, respectively, as

$$U = U_{\text{pol}} + U_{\text{es}} + U_{\text{rd}} \tag{8}$$

The form of U_{pol} is given by eqs 3 and 7. To evaluate the polarization energy, atomic point polarizabilities are required and were determined in an iterative manner. Given the ab initio polarizability tensor, calculated in NWChem[46] at the CCSD-(T)/aug-cc-pVQZ level of theory:

$$\hat{\alpha}_{N_2} = \begin{pmatrix} 1.4982 & 0 & 0 \\ 0 & 1.4982 & 0 \\ 0 & 0 & 2.1640 \end{pmatrix} \text{Å}^3 \tag{9}$$

one constructs a model tensor via the Thole polarization model in attempt to match the ab initio tensor. Initial values for point polarizabilities were chosen from a carefully constructed training set, developed by van Duijnen et al.[43] Through refinement, the ab initio tensor, that itself is in agreement with experimental measurements of the trace,[28] was exactly reproduced. The atomic point polarizabilities which gave the best fit to $\hat{\alpha}_{N_2}$ are α_{N2A} = 0.4551 Å^3 and α_{N2C} = 1.4965 Å^3 (respectfully corresponding to the atom-centered and center-of-mass sites, as illustrated in Figure 2). Note that modeling without induction amounts to setting $U_{\text{pol}} = 0$, and when this is the case our model is referred to as N_2-PHAST (nonpolar), whereas N_2-PHAST* signifies the inclusion of polarization, as stated. Constructing a model neglecting explicit polarization (the N_2-PHAST model has some measure of two-body polarization implicit in the potential) is useful for widely employed simulation codes and appropriate when strong charge interactions are less relevant. N_2-PHAST is also useful as a negative control in modeling phenomena, such as sorption in polar media, in which case it can provide a metric for the degree of substrate polarization.

Figure 2 provides a visual description of the five-site nitrogen model. Two sites, labeled N2A, are atom-centered. A third site, denoted N2C, is positioned at the molecule's center. Both the N2A and N2C sites have associated charge and polarization parameters. Additionally, the N2C site contains a Lennard-Jones ε and σ value. The remaining two sites, named N2F, reside at the extremes of the molecule and are Lennard-Jones sites. Note, the only mass-containing sites are those of the N2A type.

Further deconstructing the potential energy function piecewise, the electrostatic energy term U_{es} is parametrized to reproduce the quadrupole−quadrupole interactions between nitrogen molecules. The ab initio molecular electric quadrupole tensor was calculated at the CCSD(T)/aug-cc-pV5Z level of theory via the finite-field method[47] and found to be $\Theta = -1.514$

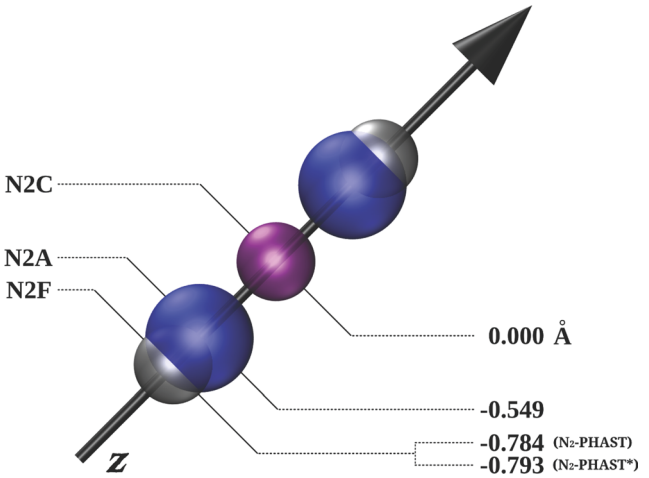

Figure 2. A diagrammatic five-site N_2 monomer, indicating the positions (values in Å) of the three different sites: N2C (purple), N2A (blue), and N2F (gray). Note the only positional difference between the nonpolar (N_2-PHAST) and polar (N_2-PHAST*) model is observed in the N2F site, where the nonpolar site resides slightly closer to the molecule's center relative to the polar N2F site. The site locations illustrated above are those obtained when implementing the WH mixing rules, though the analogous LB positions differ minutely. All potential parameters are listed in Table 1.

DÅ, which is in very good agreement with experiment.[28,48−51] A homogeneous field strength of 0.005 au was found to be effective after careful refinement and is consistent with values used by others.[52] The expression for the quadrupole moment of an axially symmetric molecule aligned along the z-axis is[53]

$$\Theta \equiv \Theta_{zz} = \sum_i e_i z_i^2 \tag{10}$$

Establishment of appropriate partial charges for the N2A and N2C sites requires a consideration of the N_2 electrostatics. Given the calculated permanent quadrupole moment and the positions of the nitrogen nuclei ($z = \pm 0.549$ Å), rearrangement of eq 10 gives atomic charges that reproduce the first nonvanishing multipole moment, by construction. To parametrize the potential form, the partial charges were allowed to float, through a simulated annealing process in parameter space, along with the other potential parameters in seeking an overall best mapping to the high-level reference surface.[18] Initial charge values reproduced the permanent quadrupole at the Hartree−Fock level of theory (which is also negative, with about 20% smaller magnitude), and the resulting charges reproduced the CCSD(T) quadrupole moment to within 0.2%. The charges on the nitrogen atoms are then $q_{N2A,float} = -0.5237$ e, and the site at the molecule's center is assigned a charge equal to $qN2C,float = -2q_{N2A,float} = +1.0474$ e. Throughout our studies these charges have been used, therefore the "float" subscript notation shall be implied and omitted.

The electronic repulsion/dispersion contribution to the total energy, U_{rd}, is described via a Lennard-Jones 12-6 function. Pair mixing of nonidentical sites is treated via two sets of rules: Lorentz−Berthelot (LB) and Waldman−Hagler (WH).[54] The well-known LB rules estimate the well depth ε_{ij} for a mixed pair of unlike sites (ij, where $i \neq j$) as a geometric mean, and the characteristic length σ_{ij} as an arithmetic mean:

$$\varepsilon_{ij} = (\varepsilon_{ii}\varepsilon_{jj})^{1/2}$$
$$\sigma_{ij} = \frac{1}{2}(\sigma_{ii} + \sigma_{jj}) \tag{11}$$

WH proposed mixing rules that are slightly more complicated:

$$\varepsilon_{ij} = (\varepsilon_{ii}\varepsilon_{jj})^{1/2}\left(\frac{\sigma_{ii}^3\sigma_{jj}^3}{\sigma_{ij}^6}\right)$$
$$\sigma_{ij} = \left(\frac{\sigma_{ii}^6 + \sigma_{jj}^6}{2}\right) \tag{12}$$

LB mixing rules have the advantage that they are extensively tested and widely implemented. However, WH showed that their prescription was substantially more effective in reproducing mixed rare gas interactions.[54,55] The WH rules, in contrast to other more advanced schemes,[56] retain simplicity and ease of implementation. WH was also chosen because it can be shown to be consistent with a perturbative expansion of the polarizability model (eq 3) that leads to dispersion interactions in the zero field limit.[17] Note, it is required to use mixing rules even in constructing a N_2 pair potential as there are unlike sites within the proposed model (see Figure 2).

Along with the partial charges and the N2F site's position, the Lennard-Jones potential parameters ε and σ were included in the multiparameter stochastic mapping to the Born−Oppenheimer surface (Figure 1a). Note, during this process the parameters associated with U_{pol} are held fixed at the values given above. Also note that the N2F site positions were constrained to the z-axis such that the COM displacements remain equivalent, i.e., their z-components are equal in magnitude but opposite in sign.

The process was performed a total of four times, thereby resulting in four parameter sets: each model (polar and nonpolar) was treated using both sets of mixing rules (LB and WH). The potential surface illustrated in Figure 1a was

Table 1. Potential Parameters (site position (R) and Lennard-Jones ε and σ) of the Polar (N_2-PHAST*) and Nonpolar (N_2-PHAST) Models for Both the LB and WH Mixing Rules[a]

		common		LB			WH		
model	site	Q (e)	$\alpha°$ (Å^3)	R (Å)	ε/k_B (K)	σ (Å)	R (Å)	ε/k_B (K)	σ (Å)
N_2-PHAST*	N2C	1.0474	1.4965	0.000	27.0222	3.4357	0.000	31.0329	3.4047
	N2F	0.0000	0.0000	±0.791	14.5517	3.0841	±0.793	13.4780	3.0899
	N2A	−0.5237	0.4551	±0.549	0.0000	0.0000	±0.549	0.0000	0.0000
N_2-PHAST	N2C	1.0474	0.0000	0.000	25.6443	3.4442	0.000	27.2601	3.4203
	N2F	0.0000	0.0000	±0.788	15.5320	3.0729	±0.784	15.3094	3.0777
	N2A	−0.5237	0.0000	±0.549	0.0000	0.0000	±0.549	0.0000	0.0000

[a]Common parameters (charge (Q) and point polarizability ($\alpha°$)) are globally shared and therefore nonexclusive to either mixing rule schemes.

dx.doi.org/10.1021/ct400526a | J. Chem. Theory Comput. 2013, 9, 5550−5557

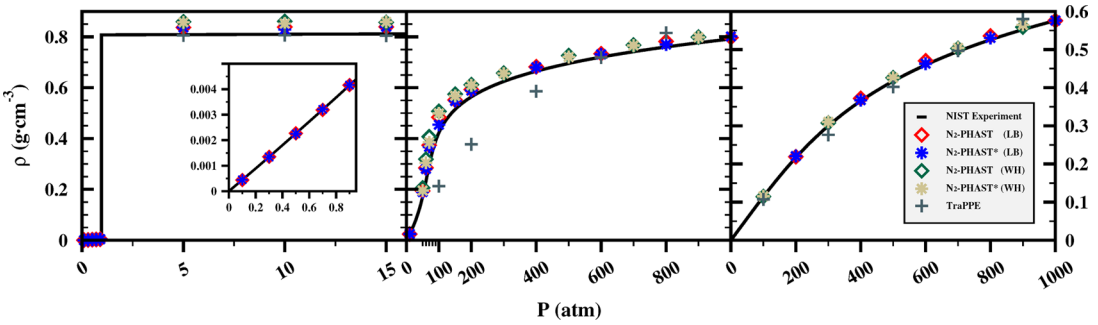

Figure 3. Pressure−density isotherms at 77 K (left), 150 K (center), and 298.15 K (right). The inset of the 77 K isotherm depicts the simulated low-pressure points of the gas phase.

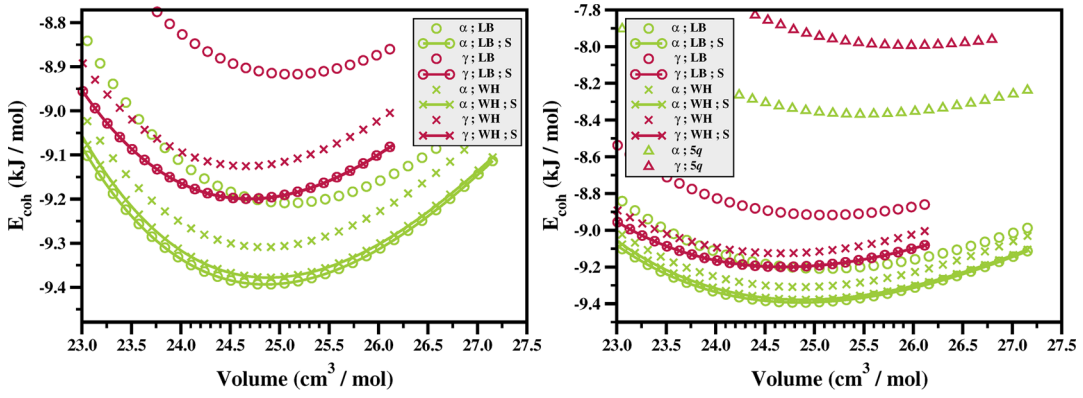

Figure 4. Calculated cohesive energies for the α-N_2 (green) and γ-N_2 (red) crystals via the N_2-PHAST* potential. (a) Comparing the two sets of mixing rules, LB and WH, a notable energy difference exists when an incomplete representative dimer set is used (symbols only). In contrast, both mixing rules trend toward the same energetics when the dimer set is more comprehensive (symbols with lines), i.e., by including the **S** configuration. (b) A wider-scaled version of (a), including the calculated energetics via the *5q* potential of Murthy.[26]

generated using the WH mixing rules. The analogous LB surface is visually indistinguishable and therefore not depicted. Table 1 provides a complete listing of the potential parameters.

Model Validation. To validate our potential, several comparisons were performed. The following experimental measurements were chosen as benchmarks: pressure−density isotherms in the vapor, supercritical, and liquid phases and the energetics and lattice constants of crystalline α-N_2 and γ-N_2. Further, thermal trimer configurations were generated, and the model energetics compared to nearly exact high-level electronic structure calculations (at the same level of theory used to generate the potential curves). Classical simulations were performed using an in-house code, MPMC,[57] which is distributed under the GNU General Public License (v3) via Google Code.

Bulk Pressure−Density Isotherms. In developing a potential effective under a variety of conditions, from gas phase to highly anisotropic sorption environments, a first step is validating its neat, bulk behavior. Thermodynamic averages were collected, and pressure−density isotherms constructed, for bulk systems over a large region of phase space and compared to experiment. Simulations were performed using the isothermal−isobaric (NPT) ensemble, and all experimental data were obtained from the Thermophysical Properties of Fluid Systems database of the NIST Web book.[58]

At 77 K, simulations were performed at pressures up to 15 atm. The resulting isotherm, plotted against experiment, is shown in Figure 3. Note that a phase transition (vapor → liquid) is experimentally observed at 0.96 atm and that our potential captures the densities well on either side. It is important to test our potential in this neighborhood of phase space not only to ensure that the potential accurately captures the transition and existence in the liquid phase but also because this is representative of nitrogen loading in MOFs; liquid nitrogen is used to conveniently and inexpensively characterize pore volume/size at 77 K. Exploring deeper into the liquid phase, one additional simulation was performed at 100 K/100 atm (not shown). All models calculated densities to within 5% of experiment at this state point.

Isothermal pressure−density plots were also constructed at 150 and 298.15 K and are illustrated in Figure 3. For both temperatures, the potentials are validated up to 1000 atm and maintain excellent agreement with experiment throughout. Note the sigmoidal shape of the 150 K isotherm, indicative of a dense supercritical fluid (T_C = 126.192 K, P_C = 33.514 atm, ρ_C = 0.3133 g·cm^{-3}).[58]

Included in the plots within Figure 3 are pressure−density data for the three-site nonpolar TraPPE[22] model. TraPPE was designed for use in liquid simulations, and thus it is no surprise that it performs very well at 77 K. Similarly, its prediction of densities at 298.15 K is relatively good. At 150 K, however, it is not as accurate. As exemplified in each plot within Figure 3, all models (LB/WH in combination with N_2-PHAST/PHAST*) performed equally well at all simulated temperatures and pressures.

Solid Phase. To test the transferability of our compact potential form, crystal lattice parameters and associated energetics were calculated for nitrogen in the alpha (α-N_2)

Table 2. Calculated α-N_2 and γ-N_2 Lattice Parameters for Both the Polar (N_2-PHAST*) and Nonpolar (N_2-PHAST) Models As Well As Both the LB and WH Mixing Rules[a]

		α-N_2				γ-N_2					
mixing rule	model	a_{calc}	a_{exp}	Vol_{calc}	Vol_{exp}	a_{calc}	a_{exp}	c_{calc}	c_{exp}	Vol_{calc}	Vol_{exp}
LB	N_2-PHAST*	5.486	5.644	24.86	27.07	3.990	3.957	5.152	5.109	24.70	24.09
	N_2-PHAST	5.483	5.644	24.82	27.07	3.987	3.957	5.148	5.109	24.64	24.09
WH	N_2-PHAST*	5.488	5.644	24.88	27.07	3.990	3.957	5.152	5.109	24.70	24.09
	N_2-PHAST	5.485	5.644	24.84	27.07	3.989	3.957	5.150	5.109	24.68	24.09
	Murthy 5q	5.532	5.644	25.49	27.07	4.057	3.957	5.238	5.109	25.96	24.09

[a]Also included is the 5q model of Murthy.[26] The experimental α phase lattice constant, a_{exp}, was reported by Wyckoff.[65] All lattice parameters are reported in units of Å and volumes in cm^3/mol.

and gamma (γ-N_2) solid phases. Both phases have been examined theoretically[26,59−62] and experimentally.[63−69] Figure 4 depicts the cohesive energy[60,63,64] as a function of volume, for the various models. Further, it demonstrates the importance of including the **S** configuration in the representative set of dimers.

α-N_2. α-N_2 is the low temperature and pressure phase and thus the lowest-energy configuration. Experimentally, it is characterized as having a primitive cubic crystal structure with space group $Pa\bar{3}$, lattice constant a = 5.644 Å (at 4.2 K) and bond length equal to 1.055 Å.[63,65,66] In simulation, a crystal composed of 125 unit cells was used. The chosen N_2 bond length was 1.098 Å (representative of the gas phase) and therefore slightly longer than the experimental value. The change in bond length associated with different environments can be captured by augmenting our model with flexibility, as was done in a similar polarizable potential.[29,30]

The energy profile as a function of the lattice constant a was calculated for values ranging from 5.300 to 5.650 Å, in Δ0.001 Å increments. When using the WH parameters, the N_2-PHAST* and N_2-PHAST models captured the minimum energy at a = 5.488 Å and a = 5.485 Å, respectively; this compares favorably to within 2.8% of the experimental value. Alternatively, when the nonpolar LB parameters are used, the calculated lattice constant is slightly further from the experimental result. Comparing to the existing 5q potential of Murthy,[26] it is found that 5q more accurately predicts the lattice parameters for α-N_2, being 2% different from experiment as opposed to our best 2.8% via the N_2-PHAST* model. The equilibrium cohesive energy, however, is 1 kJ/mol greater than the minimum of our best model, as is shown in Figure 4b. Table 2 provides a complete listing of the calculated and experimental lattice constants and volumes.

Figure 4a compares the model energetics for the two different mixing rules. The α phase is represented in green. Including the **S** orientation in the representative dimer set (solid lines with symbols) results in a more stable crystal versus its exclusion (symbols only). As seen experimentally, the α phase is the most stable at zero temperature, and the magnitude of the cohesive energy is consistent with both theoretical (MP2)[60] and experimentally derived estimates.[63,64] This is especially interesting given that the WH models, both including and neglecting the **S** configuration, give very similar dimer PESs (even for **S**, see Figure 1b), nearly identical liquid-phase results but different solid energies. Further, the convergence of the two models, i.e., LB and WH, when including a larger configuration space, is encouraging and suggests a more robust representation of the true PES.

γ-N_2. The γ crystalline lattice is tetragonal with two molecules per unit cell and is of the $P4_2/mnm$ space group. Determined by X-ray diffraction, the lattice constants are reported to be a = 3.957 Å and c = 5.109 Å for a crystal with an N_2 interatomic distance of 1.100 Å.[68]

By the same method described above for α-N_2, the energy profile of a γ-N_2 crystal as a function of volume was calculated, using all PHAST models, and the results tabulated in Table 2. Using the WH mixing rules, the calculated lattice parameters for the polar and nonpolar models, respectively, are a = 3.990 Å/c = 5.152 Å and a = 3.989 Å/c = 5.150 Å. The analogous LB parameters are little changed, with N_2-PHAST* and N_2-PHAST predicting a = 3.990 Å/c = 5.152 Å and a = 3.987 Å/c = 5.148 Å, respectively. In contrast to α-N_2, the 5q model of Murthy less accurately predicts the volume of the γ-N_2 crystal, being 7.47% different from experiment as opposed to our best 2.26% via the N_2-PHAST model with LB mixing. The minimum cohesive energy, again, is too repulsive and thus does not give an acceptable description of the energetics of either solid phase.

Similar to the trend observed in the α phase, but to a larger degree for γ, including the **S** orientation in mapping to the reference PES results in stabilization (red symbols and lines in Figure 4a). Note that in both crystalline phases, excluding the **S** configuration and modeling via the N_2-PHAST* potential using the WH mixing rules (Xs only, no lines) results in more accurate energetics compared to the LB rules. As above, it is shown that both mixing rules trend toward the same energetics as the representative dimer set becomes more comprehensive.

The present minimum, zero temperature, energy values for α and γ nitrogen are comparable within expected uncertainties from experiments and MP2 calculations. Exact comparison to experiment is difficult due to needed zero-point corrections and thermal effects that have significant errors compared to the small energy differences considered. The comparison with theoretical MP2 calculations is also limited by uncertainties associated with this level of perturbative analysis.[60,64,70] For reference, an estimate of the zero-point corrected cohesive energy of α nitrogen was given as −8.3 kJ/mol;[60] this is reasonably close to our model calculation. Note, the calculations presented in Figure 4 are zero temperature and, in that sense, represent a lower bound to the energy. Further, distinct calculations have found the energy difference between the α and γ phases to be comparably small.[60,64] Again, note that the N_2-PHAST model bond length is taken as the gas phase value which differs from the observed crystalline value by nearly 4%. This can also have a small nonnegligible effect on the energetics.[60] The general agreement between our model solids and experimental data is also inspiring given the small magnitude of energy involved, which requires a high-fidelity representation of the PES. The solid−solid transition line is not calculated in this work as the focus of this potential is for use in

heterogeneous media, however might be of interest in future studies.

Trimer Energetics. A final test was performed, comparing thermal trimer configurations to nearly exact electronic structure calculations on the same configuration. This test involves (minimal) many-body contributions and explores a relatively wide region of configuration space, while still allowing rigorous detailed comparison. An ensemble of 100 three-molecule configurations were generated via Monte Carlo (using N_2-PHAST) at 15 K, effectively exploring the PES while avoiding dissociation. Single-point energy calculations were then performed for each configuration subject to each potential of interest: N_2-PHAST* and N_2-PHAST, with LB and WH mixing rules. Ab initio single-point calculations were then performed for each configuration at the CCSD(T) level of theory using aug-cc-pVTZ/QZ with CBS extrapolation.

Taking the CCSD(T) value as exact, the root-mean-square error (RMSE) in single-point energy over the ensemble was calculated. The results are plotted in Figure 5. For the two LB

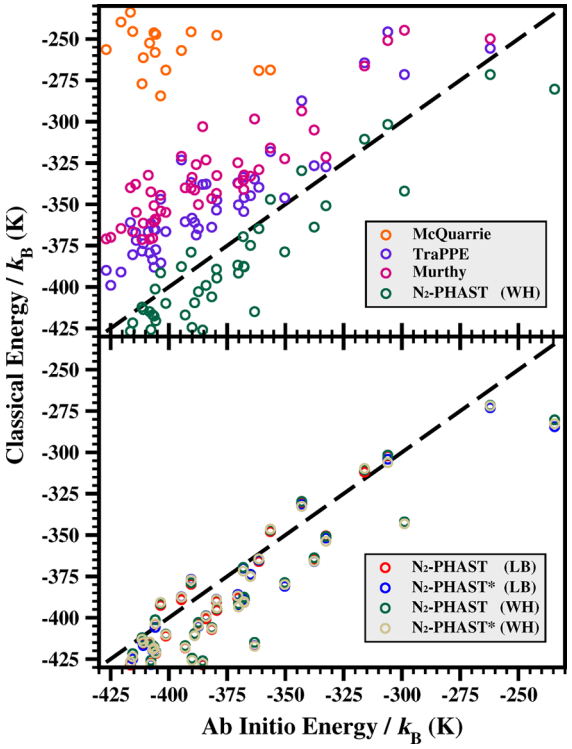

Figure 5. The classical potential energy function is compared to the ab initio values for an ensemble of 100 trimers (circles). Data points in perfect agreement would fall along the dashed line.

potentials, values of 6.84% and 6.81% were found for N_2-PHAST* and N_2-PHAST, respectively. For the WH potentials, values of 6.85% and 6.51% were found. In both cases, adding polarization to the potential was not found to significantly affect the accuracy of trimer energy calculations. All of the potentials from this work perform markedly better than comparable potentials from other works in the context of this test. A calculation using the 5*q* potential of Murthy over the ensemble produced a RMSE of 13.26%, the three-site nonpolar TraPPE[22] potential produced an error of 9.41% and the single-site isotropic model by McQuarrie,[71] unsurprisingly, produced an error of 56.59%. These results are represented by pink, purple, and orange data sets, respectively, in Figure 5. It can be seen that the 5*q* potential gives a reasonably good result comparable to that of TraPPE but with slightly more systematic error.

CONCLUSIONS

Using five high-level reference ab initio curves, a five-site anisotropic and transferable potential energy function for N_2 has been developed. Two potential models, one including (N_2-PHAST*) and one neglecting (N_2-PHAST) explicit induction effects, have been defined. Additionally, two differing sets of mixing rules (LB and WH) are used. The combination of each model with mixing rule results in four total parameter sets. All have been extensively tested and proven accurate for bulk systems across a wide region of phase space, encompassing the condensed, vapor, and supercritical phases. Pressure−density isotherms were constructed at 77, 150, and 298.15 K and closely reproduce experiments in all explored regions of phase space. Thermal trimer and solid-state energetics were calculated and successfully tested the transferability of the defined potential models.

Including an ostensibly redundant dimer orientation, the **S** configuration, led to a more robust PES. Further, only with the improved surface did both sets of mixing rules give similar solid energetics. This suggests mapping the PES to carefully chosen stochastic sets of dimer configurations to exhaustively explore configuration space, and this approach[39] will be pursued in the future.

AUTHOR INFORMATION

Corresponding Author

*E-mail: ccioce@mail.usf.edu

Notes

The authors declare no competing financial interest.

ACKNOWLEDGMENTS

Financial support from the National Science Foundation (grant no. CHE-1152362) is gratefully acknowledged. Computations were performed on the following XSEDE resources (TG-DMR090028): PSC Blacklight, TACC Ranger, and SDSC Trestles. Local computations were performed at the USF Research Computing Center, where NSF-funded computational resources (under grant no. CHE-0722887) were greatly appreciated. The authors would also like to thank A. Erba for our communications and his willingness to share data.

REFERENCES

(1) Snurr, R. Q.; Hupp, J. T.; Nguyen, S. T. *AIChE J.* **2004**, *50*, 1090−1095.
(2) Delgado, J. A.; Uguina, M. A.; Gómez, J. M.; Ortega, L. *Sep. Purif. Technol.* **2006**, *48*, 223−228.
(3) Moulton, B.; Zaworotko, M. J. *Chem. Rev.* **2001**, *101*, 1629−1658.
(4) Farha, O. K.; Özgür, A. Yazaydn; Eryazici, I.; Malliakas, C. D.; Hauser, B. G.; Kanatzidis, M. G.; Nguyen, S. T.; Snurr, R. Q.; Hupp, J. T. *Nat. Chem.* **2010**, *2*, 944−948.
(5) Eddaoudi, M.; Moler, D. B.; Li, H.; Chen, B.; Reineke, T. M.; O'Keeffe, M.; Yaghi, O. M. *Acc. Chem. Res.* **2001**, *34*, 319−330.
(6) Zheng, B.; Bai, J.; Duan, J.; Wojtas, L.; Zaworotko, M. J. *J. Am. Chem. Soc.* **2011**, *133*, 748−751.
(7) Mohamed, M. H.; Elsaidi, S. K.; Wojtas, L.; Pham, T.; Forrest, K. A.; Tudor, B.; Space, B.; Zaworotko, M. J. *J. Am. Chem. Soc.* **2012**, *134*, 19556−19559.
(8) Nugent, P.; Belmabkhout, Y.; Burd, S.; Cairns, A.; Luebke, R.; Forrest, K.; Pham, T.; Ma, S.; Space, B.; Wojtas, L.; Eddaoudi, M.; Zaworotko, M. *Nature* **2013**, *495*, 80−84.

(9) Britt, D.; Furukawa, H.; Wang, B.; Glover, T. G.; Yaghi, O. M. *Proc. Natl. Acad. Sci. U.S.A.* **2009**, *106*, 20637−20640.
(10) Millward, A. R.; Yaghi, O. M. *J. Am. Chem. Soc.* **2005**, *127*, 17998−17999.
(11) Banerjee, R.; Phan, A.; Wang, B.; Knobler, C.; Furukawa, H.; O'Keeffe, M.; Yaghi, O. M. *Science* **2008**, *319*, 939−943.
(12) Snurr, R. Q.; Yazaydin, A. O.; Dubbeldam, D.; Frost, H. In *Molecular Modeling of Adsorption and Diffusion in Metal-Organic Frameworks*; John Wiley & Sons, Inc.: Hoboken, NJ, 2010; pp 313−339.
(13) Bock, S.; Bich, E.; Vogel, E. *Chem. Phys.* **2000**, *257*, 147−156.
(14) Hellmann, R.; Bich, E.; Vogel, E. *Proc. Natl. Acad. Sci. U.S.A.* **2008**, *128*, 2143031−2143039.
(15) Forrest, K. A.; Pham, T.; McLaughlin, K.; Belof, J. L.; Stern, A. C.; Zaworotko, M. J.; Space, B. *J. Phys. Chem. C* **2012**, *116*, 15538−15549.
(16) Pham, T.; Forrest, K. A.; McLaughlin, K.; Tudor, B.; Nugent, P.; Hogan, A.; Mullen, A.; Cioce, C. R.; Zaworotko, M. J.; Space, B. *J. Phys. Chem. C* **2013**, *117*, 9970−9982.
(17) McLaughlin, K.; Cioce, C. R.; Belof, J. L.; Space, B. *J. Chem. Phys.* **2012**, *136*, 194302.
(18) Belof, J. L.; Stern, A. C.; Space, B. *J. Chem. Theory Comput.* **2008**, *4*, 1332−1337.
(19) Belof, J. L.; Stern, A. C.; Space, B. *J. Phys. Chem. C* **2009**, *113*, 9316−9320.
(20) Mullen, A. L.; McLaughlin, K.; Cioce, C. R.; Belof, J. L.; Space, B. *J. Chem. Theory Comput.*, submitted.
(21) Cioce, C. R.; Tudor, B.; McLaughlin, K.; Belof, J. L.; Space, B. in preparation.
(22) Potoff, J. J.; Siepmann, J. I. *AIChE J.* **2001**, *47*, 1676−1682.
(23) Liu, Y.; Panagiotopoulos, A. Z.; Debenedetti, P. G. *J. Phys. Chem. B* **2011**, *115*, 6629−6635.
(24) *TraPPE Force Field and Parameter Database*; The Siepmann Group, University of Minnesota: Minneapolis, MN; http://www.chem.umn.edu/groups/siepmann/trappe/intro.php (accessed September 2013).
(25) Yu, K.; McDaniel, J. G.; Schmidt, J. R. *J. Phys. Chem. B* **2011**, *115*, 10054−10063.
(26) Murthy, C. S.; O'Shea, S. F.; McDonald, I. R. *Mol. Phys.* **1983**, *50*, 531−541.
(27) Huber, K. P.; Herzberg, G. *Molecular Spectra and Molecular Structure. IV. Constants of Diatomic Molecules*; Van Nostrand Reinhold Company: New York, 1979.
(28) *NIST Computational Chemistry Comparison and Benchmark Database, NIST Standard Reference Database Number 101*, release 15b;Johnson, R. D., III, Ed.; NIST: Gaithersburg, MD, 2011.
(29) Mankoo, P. K.; Keyes, T. *J. Phys. Chem. B* **2006**, *110*, 25074−25079.
(30) Keyes, T.; Napoleon, R. L. *J. Phys. Chem. B* **2011**, *115*, 522−531.
(31) Diep, P.; Johnson, J. K. *J. Chem. Phys.* **2000**, *112*, 4465−4473.
(32) Aquilanti, V.; Bartolomei, M.; Cappelletti, D.; Carmona-Novillo, E.; Pirani, F. *J. Chem. Phys.* **2002**, *117*, 615−627.
(33) Werner, H.-J.; Knowles, P. J.; Knizia, G.; Manby, F. R.; Schütz, M. et al. *MOLPRO*, version 2010.1, a package of ab initio programs; University College Cardiff Consultants Limited: Cardiff, U.K., 2010; see http://www.molpro.net.
(34) Raghavachari, K.; Trucks, G. W.; Pople, J. A.; Head-Gordon, M. *Chem. Phys. Lett.* **1989**, *157*, 479−483.
(35) Dunning, T. H., Jr. *J. Chem. Phys.* **1989**, *90*, 1007−1023.
(36) Kendall, R. A.; Dunning, T. H., Jr.; Harrison, R. J. *J. Chem. Phys.* **1992**, *96*, 6796−6806.
(37) Boys, S.; Bernardi, F. *Mol. Phys.* **1970**, *19*, 553−566.
(38) Huh, S. B.; Lee, J. S. *J. Chem. Phys.* **2003**, *118*, 3035−3042.
(39) Babin, V.; Medders, G. R.; Paesani, F. *J. Phys. Chem. Lett.* **2012**, *3*, 3765−3769.
(40) Sundberg, K. *J. Chem. Phys.* **1977**, *66*, 114.
(41) Bode, K. A.; Applequist, J. *J. Phys. Chem.* **1996**, *100*, 17820−17824.
(42) Thole, B. *Chem. Phys.* **1981**, *59*, 341−350.
(43) van Duijnen, P. T.; Swart, M. *J. Phys. Chem. A* **1998**, *102*, 2399−2407.
(44) Yonezawa, Y. *J. Chem. Phys.* **2012**, *136*, 244103.
(45) Tudor, B.; Space, B. *J. Comput. Sci. Ed.*, submitted.
(46) Valiev, M.; Bylaska, E.; Govind, N.; Kowalski, K.; Straatsma, T.; Dam, H. V.; Wang, D.; Nieplocha, J.; Apra, E.; Windus, T.; de Jong, W. *Comput. Phys. Commun.* **2010**, *181*, 1477−1489.
(47) Cohen, H. D.; Roothaan, C. C. J. *J. Chem. Phys.* **1965**, *43*, S34−S39.
(48) Graham, C.; Imrie, D. A.; Raab, R. E. *Mol. Phys.* **1998**, *93*, 49−56.
(49) Huot, J.; Bose, T. K. *J. Chem. Phys.* **1991**, *94*, 3849−3854.
(50) Roco, J. M. M.; Hernández, A. C.; Velasco, S.; Medina, A. *J. Chem. Phys.* **1999**, *110*, 5218−5223.
(51) Buckingham, A.; Graham, C.; Williams, J. *Mol. Phys.* **1983**, *49*, 703−710.
(52) Maroulis, G. *J. Chem. Phys.* **2003**, *118*, 2673−2687.
(53) Buckingham, A. D. *Q. Rev. Chem. Soc.* **1959**, *13*, 183−214.
(54) Waldman, M.; Hagler, A. *J. Comput. Chem.* **1993**, *14*, 1077−1084.
(55) White, A. Intermolecular Potentials of Mixed Systems: Testing the Lorentz-Berthelot Mixing Rules with Ab Initio Calculations. *DSTO Aeronautical and Maritime Research Laboratory Technical Report DSTO-TN-0302*; DSTO Aeronautical and Maritime Research Laboratory: Melbourne, Australia, 2000.
(56) Al-Matar, A. K.; Rockstraw, D. A. *J. Comput. Chem.* **2004**, *25*, 660−668.
(57) *Massively Parallel Monte Carlo (MPMC)*. MPMC is an in-house code developed by Jonathan Belof and maintained by Keith McLaughlin, Christian R. Cioce, Brant Tudor, and Adam Hogan. MPMC is released under GNU Public License and is available on Google Code http://code.google.com/p/mpmc.
(58) Lemmon, E.; McLinden, M.; Friend, D. In *NIST Chemistry WebBook, NIST Standard Reference Database Number 69*; Linstrom, P.; Mallard, W., Eds.; National Institute of Standards and Technology: Gaithersburg, MD, 2005.
(59) Kuan, T.-S.; Warshel, A.; Schnepp, O. *J. Chem. Phys.* **1970**, *52*, 3012−3020.
(60) Erba, A.; Maschio, L.; Salustro, S.; Casassa, S. *J. Chem. Phys.* **2011**, *134*, 074502.
(61) van der Avoird, A.; Wormer, P. E. S.; Jansen, A. P. J. *J. Chem. Phys.* **1986**, *84*, 1629−1635.
(62) Mulder, A.; Michels, J. P. J.; Schouten, J. A. *J. Chem. Phys.* **1996**, *105*, 3235−3244.
(63) Scott, T. A. *Phys. Rep.* **1976**, *27*, 89−157.
(64) Jordan, P. C.; van Maaren, P. J.; Mavri, J.; van der Spoel, D.; Berendsen, H. J. C. *J. Chem. Phys.* **1995**, *103*, 2272−2285.
(65) Wyckoff, R. W. G. In *Crystal Structures*; John Wiley & Sons: Hoboken, NJ, 1963; Vol. *1*, pp 29−30.
(66) *Crystal Data Determinative Tables*; Donnay, J. D. H.; Donnay, G., Eds., 2nd ed.; American Crystallographic Association: Buffalo, NY, 1963; p 884.
(67) Raich, J. C.; Mills, R. L. *J. Chem. Phys.* **1971**, *55*, 1811−1817.
(68) Mills, R. L.; Schuch, A. F. *Phys. Rev. Lett.* **1969**, *23*, 1154−1156.
(69) Schuch, A. F.; Mills, R. L. *J. Chem. Phys.* **1970**, *52*, 6000−6008.
(70) Pickard, C. J.; Needs, R. J. *Phys. Rev. Lett.* **2009**, *102*, 125702.
(71) McQuarrie, D. A.; Simon, J. D. In *Physical chemistry: a molecular approach*; University Science Books: Sausalito, CA, 1997; p 663.